Generation of highly anisotropic physical properties in ferromagnetic thin films controlled by their differently oriented nano-sheets

Cite as: AIP Advances 14, 025237 (2024); doi: 10.1063/9.0000813
Submitted: 4 October 2023 • Accepted: 10 January 2024 •
Published Online: 20 February 2024

View Online Export Citation CrossMark

C. Favieres,[1,2,a)] J. Vergara,[1,2] C. Magén,[3,4,5] M. R. Ibarra,[3,4,5] and V. Madurga[1]

AFFILIATIONS

[1] Laboratorio de Magnetismo, Departamento de Ciencias, Física, Universidad Pública de Navarra (UPNA), Campus de Arrosadía, Pamplona, España
[2] Instituto de Materiales Avanzados y Matemáticas (INAMAT^2), Universidad Pública de Navarra (UPNA), Campus de Arrosadía, E-31006 Pamplona, España
[3] Instituto de Nanociencia y de Materiales de Aragón (INMA), CSIC-Universidad de Zaragoza, Zaragoza, España
[4] Departamento de Física de la Materia Condensada, Universidad de Zaragoza, Zaragoza, España
[5] Laboratorio de Microscopías Avanzadas (LMA), Universidad de Zaragoza, 50018 Zaragoza, España

Note: This paper was presented at the 68th Annual Conference on Magnetism and Magnetic Materials.
[a)] **Author to whom correspondence should be addressed:** favieresc@unavarra.es

ABSTRACT

We fabricated ferromagnetic nano-crystalline thin films of Co, Fe, Co–Fe and Co-rich and Fe-rich, Co–MT and Fe–MT (MT = transition metal), constituted by nano-sheets with a controlled slant. Visualization of these nano-sheets by Scanning Tunneling Microscopy and High-Resolution Transmission Electron Microscopy (HRTEM) showed typically tilt angles ≈56° with respect to the substrate plane, and nano-sheets ≈3.0–4.0 nm thick, ≈30–100 nm wide, and ≈200–300 nm long, with an inter-sheet distance of ≈0.9–1.2 nm, depending on their constitutive elements. Induced by this nano-morphology, these films exhibited large uniaxial magnetic anisotropy in the plane, the easy direction of magnetization being parallel to the longitudinal direction of the nano-sheets. In the as-grown films, typical values of the anisotropy field were between $H_k \approx 48$ and 110 kA/m depending on composition. The changes in the nano-morphology caused by thermal treatments, and hence in the anisotropic properties, were also visualized by HRTEM, including chemical analysis at the nano-scale. Some films retained their nano-sheet morphology and increased their anisotropies by up to three times after being heated to at least 500 °C: for example, the thermal treatments produced crystallization processes and the growth of CoV and CoFe magnetic phases, maintaining the nano-sheet morphology. In contrast, other annealed films, Co, Fe, CoZn, CoCu. . . lost their nano-sheet morphology and hence their anisotropies. This work opens a path of study for these new magnetically anisotropic materials, particularly with respect to the nano-morphological and structural changes related to the increase in magnetic anisotropy.

© 2024 Author(s). All article content, except where otherwise noted, is licensed under a Creative Commons Attribution (CC BY) license (http://creativecommons.org/licenses/by/4.0/). https://doi.org/10.1063/9.0000813

I. INTRODUCTION

The generation and control of magnetic anisotropy at the nano-scale in thin films is a key issue to address applications in different fields, including sensors, actuators, permanent magnets, magneto-electronics, information processing or storage devices.[1–9] Magnetic materials exhibit magnetic properties that are highly dependent on their size, structure and morphology.[10–14] Considerable attention has therefore been paid to the control of these characteristics by fabrication techniques. Among them, oblique-angle incidence techniques are well-suited for this purpose. It was demonstrated that oblique deposition induces uniaxial in-plane magnetic anisotropy (UMA) in thin films.[11,12,15–30] In the pioneering works of Knorr and Hoffman[15] and Smith *et al.*,[16] they irrefutably demonstrated that the

07 March 2024 09:07:32

UMA present in evaporated Fe thin films depended on the angle the incident flux of metallic vapor made with the normal to the substrate: with inclination of the vapor to the normal there was a clear UMA; with normal incidence, the films were magnetically isotropic in their plane. These films developed a fiber axis structure due to the tilted direction of incidence of the metallic flux with respect to the normal to the substrate. In Permalloy evaporated films, Smith *et al.* correlated magnetic anisotropy with chains of crystallites whose long axes were perpendicular to the beam direction during growth. The easy axis for the magnetization was parallel to those long axes. They attributed the origin of the magnetic anisotropy to the "self-shadowing" mechanism. Since then, different oblique incidence methods, evaporation,[31] molecular beam epitaxy,[32] sputtering[11,12,20] or Pulsed Laser Deposition (PLD)[21–29,33–35] have been used for the growth of thin films exhibiting such magnetic anisotropy.

We successfully fabricated and studied ferromagnetic nanocrystalline thin films formed by nano-sheets with a controlled tilt using a particular home-made oblique-incidence PLD system. Films were grown with this distinctive nano-morphology, hereafter denominated Cylindrical Symmetry Oblique Growth (CSOG) films.[21–29] By visualization of these nano-sheets by High-Resolution Transmission Electron Microscopy (HRTEM) and Scanning Tunneling Microscopy (STM)[25–27] we discovered tilt angles ≈56° with respect to the substrate plane, and nano-sheets ≈3.0–4.0 nm thick, ≈30–100 nm wide, and ≈200–300 nm long, with an inter-sheet distance of ≈0.9–1.2 nm, depending on their constitutive elements. This tilted nano-morphology resulted in a large UMA, the easy direction of magnetization being parallel to the longitudinal direction of the nano-sheets and the hard direction being perpendicular to the longitudinal direction of the nano-sheets. In the as-grown films, typical values of the anisotropy field were between H_k = 600 and 1400 Oe (≈48 and 110 kA/m) depending on composition. The deduced effective shape anisotropy constant associated with the nano-sheets was, in some cases, similar to or even higher than the magnetocrystalline anisotropy constant. These nano-sheets were formed during the growth of the samples due to the special position of the substrates with respect to the direction of the plasma. Indeed, they were placed on the lateral surface of a cone with its axis of rotational symmetry parallel to the plasma flux direction. It caused that the growth direction of our films (always occurring towards the plasma source) retained a constant angle with respect to the direction of growth of the film observed in previous stages; i.e., with the rotation symmetry axis of the cone coincident with the cylindrical symmetry axis of the plasma flux, the film's growth direction was always preserved. This fact, together with the self-shadowing effect, allowed for the nano-sheet to be formed. This behavior was observed for the case in which the cone was rotated as well as that in which it remained static. Figure 1 shows a schematic of the substrate-holder designed in our laboratory for the growth of CSOG thin films.

In the works of other authors in which the substrate was located on a plane surface whose normal was not parallel to the plasma flux direction, and this substrate being rotated around this normal axis, the growth direction of the film (also always towards the plasma source) changed with respect to the direction of growth of the film observed in previous stages because the rotation of the substrate.[17,36–38] This is the procedure required to form nanocolumns, either with a zig-zag, multiple zig-zag or spiral structure,[36] and it occurs because the axis of the cylindrical symmetry of the rotating substrate is not coincident with the cylindrical symmetry axis of the plasma flux. Thus, the nano-morphology of our CSOG films was different from that found in other samples grown by oblique-incidence.[36–38] To name a few examples: in-plane anisotropy fields between 100 and 300 Oe were measured in oblique-deposited FeCoB: this anisotropy was attributed to a columnar shape anisotropy.[12] For Fe deposited by oblique e-beam evaporation,[18] images showed columnar Fe films and their hysteresis loops revealed that, due to the columnar growth, there was in-plane anisotropy with the in-plane easy axis parallel to the column growth direction. As well, for oblique PLD of FeGa films,[35] although in-plane magnetic anisotropy was observed, its value was considerably smaller (≈275 Oe) than that exhibited by our CSOG films and the magnetization processes in the hard direction exhibited non-zero values of the coercive field. More examples of the magnetic anisotropy exhibited by samples with nano-columns obtained by oblique deposition are given in Refs. 39 and 40 (and in references herein), demonstrating their different magnetization processes compared to those of our CSOG films, because of the different nano-morphology. Besides, the nano-column diameter varies between 20 and 60 nm,[39] significantly larger than the width of our nano-sheets (≈3–6 nm).

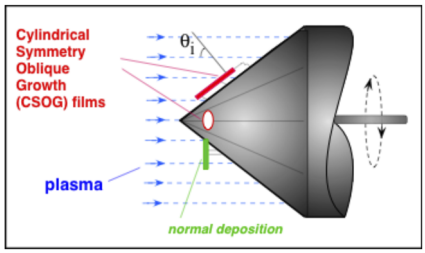

FIG. 1. Schematic of the substrate-holder designed in our laboratory for the fabrication of cylindrical symmetry oblique growth CSOG films. The substrates were placed on the lateral surface of a cone with its axis of rotational symmetry parallel to the plasma flux direction.

In this work, we review our findings on the magnetic properties of these CSOG films as well as their relation with their structure, morphology and transport properties, also presenting new results. The changes in the nano-morphology of these films caused by thermal treatments, and hence in their anisotropic properties, are also reviewed. HRTEM allowed the observation of these morphological changes. Remarkably interesting, we show that some films retain their nano-sheet morphology and maintain their anisotropies after being treated at high temperatures.

II. EXPERIMENTAL PROCEDURES

Thin films of Co, Fe, Co–Fe, and Co- and Fe-rich, Co(or Fe)–MT (MT = V, Cr, Cu, Zn, Cd, Hf, Al) were grown by PLD. A Litron Nd–YAG laser (λ = 1064 nm, 20 Hz repetition rate, 5 ns pulse and an energy of 220 mJ/pulse in the target's spot, laser fluence ≈1.8 J·cm^{-2}) and a customized Kurt J. Lesker stainless-steel chamber at a base pressure of 10^{-6} mbar were used. The films were deposited over glass substrates (7 mm in diameter and 0.13 mm thick) placed in the home-made substrate-holder shown in Fig. 1. They were placed on the lateral surface of a cone rotating at 72 rpm around its cylindrical symmetry axis; this axis was parallel to the plasma direction, and

07 March 2024 09:07:32

© Author(s) 2024

the normal to its lateral surface formed an angle of $\theta_i = 55°$ with the plasma direction. This arrangement produced the so called CSOG films. Simultaneously, other samples were perpendicularly deposited (with the plasma arriving perpendicular to the substrate, $\theta_i = 0°$). This allowed to compare the properties of both types of samples. The rotation of the cone at 72 rpm ensured a homogeneous distribution of the deposited material from the plasma. All of them were placed at distances between 60 and 70 mm from the target. Films thickness was ≈40–60 nm. A 0.4 nm Au capping layer was deposited on top of all samples to prevent oxidation.

Different rotating (32 rpm) targets were used: (1) a "mixed" target consisting of two foils, one above the other. The bottom foil was the metal MT and the top foil was either a Co or Fe foil in which circular holes, all with the same diameter, were made and uniformly distributed on the Co (or Fe) foil surface. The area corresponding to the MT, which was that corresponding to the holes, was 14% of the total target's area. During PLD, the laser's spot always reached both foils of Co (or Fe) and MT simultaneously, with an angle of 45 deg. Therefore, after the laser impact, a mixture of Co (or Fe) and MT was ejected simultaneously toward the substrates. (2) The second type of substrate was an alloyed target of Co_{100-x}–Fe_x: starting from the pure elements Co and Fe, different alloys of 25 mm in diameter and 5 mm thick were prepared. The high-purity elements in powder form were mixed, pressed, and melted at 1650 °C in a home-made furnace. The pressed pellets were melted several times to ensure complete formation of the alloy. (3) The third type of target, 25 mm in diameter, consisted of two circular sectors of Co (or Fe) and other metal MT. We labeled the films as Co_{100-x}–MT_x (or Fe_{100-x}–MT_x) where x was the area of the MT sector (typically Cu, V, Al) with respect to the total area of the target. Based on our previous works, a target revolving 32 turns per min ensured that the target composition transferred sufficiently well to the deposited films. It is also known that stoichiometry can be preserved in PLD by controlling parameters such as laser fluence, substrate temperature background gas pressure, etc.[41–43] Before each deposition, the targets were mechanically polished to always initiate the ablation–deposition under the same conditions, since the surface of the target influences the morphological and structural properties of the films.[41,44]

The surface nano-morphology of the samples was observed by STM with a Nanotec microscope and a Nanotec software.[45]

HRTEM studies were performed in an image-corrected Thermo Fisher Titan Cubed 60–300, operated at 300 kV. Cross-sectional specimens were prepared for HRTEM observations by mechanical polishing and Ar + ion milling. Electron Energy Loss Spectroscopy, EELS, at nanoscale was also performed from the cross-sectional prepared samples.

Magnetic hysteresis loops at room temperature were measured by a Vibrating Sample Magnetometer (VSM) (EG & G).

The electrical resistance, R, of the films was determined using a laboratory-made system.[29] R was always measured in the plane of the films. The sample-holder allowed the sample to be rotated with respect to an axis perpendicular to its plane, obtaining R as a function of the angle formed by the electrical current with the longitudinal direction of the expected nano-sheets. It allowed measuring its angular dependence and observing its anisotropic property. R was measured between two contacts (1 mm in diameter) separated by 4.5 mm.

The samples were structurally, magnetically and electrically characterized in the as-grown state and after being heated in a dynamic Ar atmosphere at up 500 °C in a customized furnace at a heating rate of 10 °C·min^{-1}. Once this temperature was reached, the films were removed from the hot region of the furnace and kept in the Ar atmosphere until they were slowly cooled.

III. RESULTS AND DISCUSSION

The XRD analysis of the as-grown films showed that the films had an amorphous or nano-crystalline structure, regardless of the type of target, with an ensemble of nanograins measuring 1 and 2 nm,[25–29] exhibiting broad halos. In the Co, Fe, Co–Fe, Co–V and Co–Cr films no crystalline peaks were detected. In some films, Co–Zn, Co–Cd, Co–Hf or Co–Cu films, some small peaks corresponding to Zn, Cd, Hf and Cu respectively were also detected along with the broad halo.[25]

Irrespective of the films composition, the observation of the surface morphology of the as-grown films revealed the presence of nano-strings-like structures. These nano-structures were always generated perpendicular to the incidence plane of the plasma during deposition.[21–29] Our first observations were made in Co films.[21] The average width of the nano-strings depended on the film's thickness. These special surface morphology was also observed in Fe, Co–Fe, Co–V, Co–Zn and Co–Cu samples.[27–29] We previously demonstrated that no surface nano-strings were formed in normally deposited samples irrespective of sample composition or constitutive elements, but a random distribution of grains: nano-strings were exclusive to the CSOG films.[21,28] Fig. 2 shows the STM surface observations of a Fe–Al sample (obtained from a target formed by two sectors, Fe_{90}–Al_{10}).

An important achievement was made with the discovery of the inner morphology of the CSOG films. The first results were obtained in Co films:[25,26] HRTEM studies revealed that they were formed by a set of oblique nano-sheets, 4–12 nm thick, ≈70 nm wide and ≈200–300 nm long, with an inter-sheet distance of ≈2 nm, Fig. 3(a). These nano-sheets were oriented perpendicular to the incidence plane of the plasma at an angle between 55 and 65 deg with respect to the substrate plane. Figure 3(b) is a magnification of the cross-sectional corresponding to this Co film where the black regions, with high density of atoms and nano-crystals, correspond to the nano-sheets of the film and the white regions with much lower density of atoms, correspond to the inter-nano-sheet regions. Similarly, Figs. 3(c) and 3(d), show that CSOG Co–V and Co–Zn films were formed by oblique nano-sheets: for Co–V the dimensions

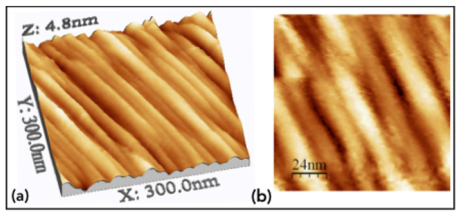

FIG. 2. (a) 3D STM and (b) 2D STM surface morphology of a cylindrical symmetry oblique Growth CSOG Fe–Al film showing nano-string-like structures oriented perpendicular to the incidence plane of the plasma during deposition.

07 March 2024 09:07:32

© Author(s) 2024

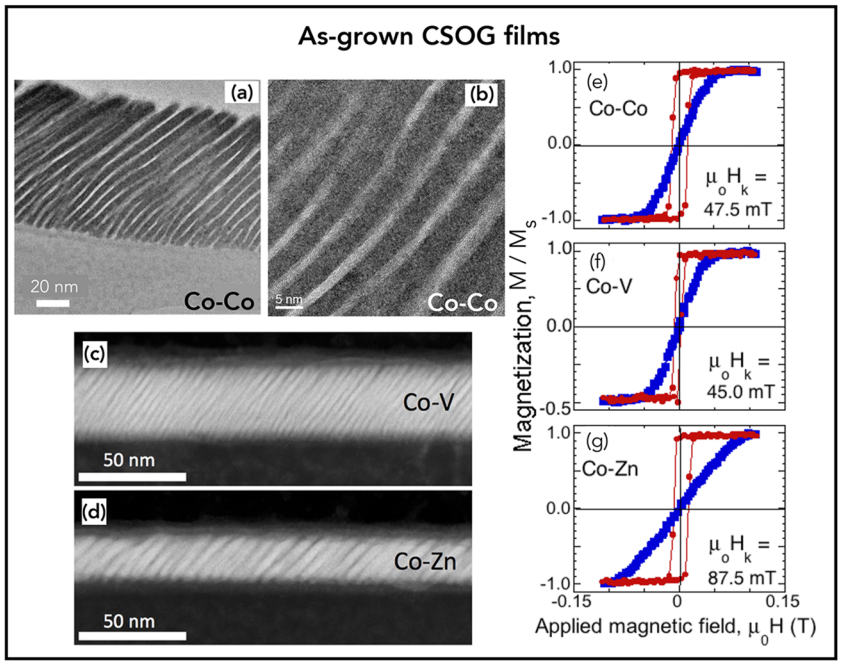

FIG. 3. High-Angle Annular Dark-Field Scanning Transmission Electron Microscopy, STEM HAADF, images of (a) and (b) Co, (c) Co–V and (d) Co–Zn CSOG films, showing the internal cross section of the nano-sheets formed during the growth of the films. In-plane *M–H* loops corresponding to the as-grown (e) Co, (f) Co–V and (g) Co–Zn films.[25,27] The hard direction (blue) and easy direction (red) are shown. Co–Co means that in the "mixed" target both foils are of Co. The easy magnetic direction was the longitudinal direction of the nano-sheets. (a), (e), (f) and (g) Adapted with permission from Favieres *et al.*, J. Alloy. Compd. **664**, 695 (2016). Copyright 2016 Elsevier. (c) and (d) Adapted with permission from Favieres *et al.*, J. Alloy. Compd. **911**, 164950 (2022); Creative Commons Attribution 4.0 International license.

were ≈3.0 nm thick and ≈40 nm wide, with an inter-sheet distance of ≈1.1 nm, and oriented perpendicular to the plane of incidence of the plasma at a tilt angle ≈53 deg; for Co–Zn, each nano-sheet was ≈4.5 nm thick, with an inter nano-sheet distance of ≈1.3 nm. The tilted nano-morphology obtained from the images of the cross section of the films and the nano-strings on their surface (as these observed in Fig. 2 and those shown in Refs. 21–29 corresponding to other compositions) were the two results that allowed to establish that our CSOG samples were composed of tilted nano-sheets.[25–27]

We showed that the as-grown CSOG films exhibited a well-defined UMA,[21–29] the easy direction of magnetization being parallel to the longitudinal direction of the nano-sheets. The magnetic

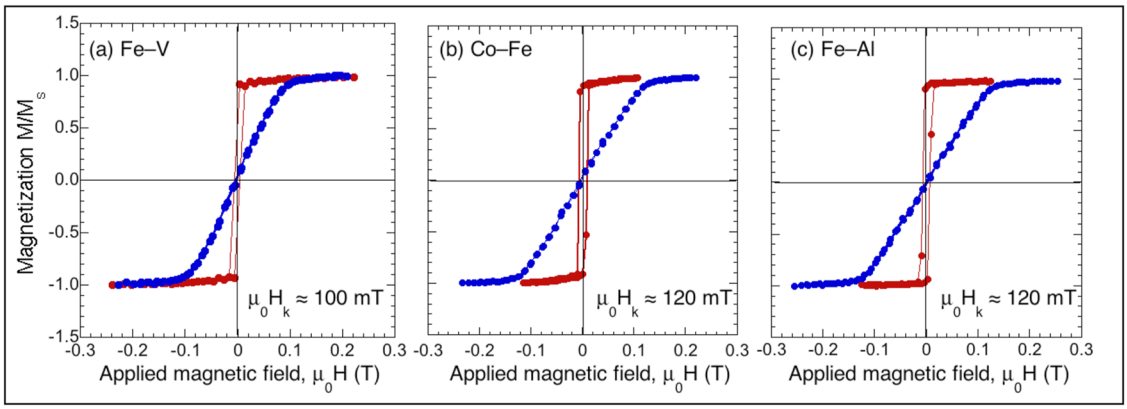

FIG. 4. M-H loops corresponding to CSOG as-grown films: (a) Fe–V obtained using a mixed target ($Fe_{86}V_{14}$, "mixed" target), (b) Co–Fe obtained using an alloyed target ($Co_{50}Fe_{50}$) and (c) Fe–Al obtained using a target of sectors ($Fe_{90}Al_{10}$). Easy magnetization direction loops (red) and hard direction loops (blue) are shown. The surface morphology with nano-strings of sample in (c) was that shown in Fig. 2.

07 March 2024 09:07:32

© Author(s) 2024

anisotropy field, H_k ($H_k = 2k/\mu_0 M_s$, with k as the anisotropy constant and $\mu_0 M_s$ as the saturation magnetization), was determined from the crossover of the hard loop. The easy direction loops were very square with almost $\mu_0 M_r/\mu_0 M_s \approx 1$, being $\mu_0 M_r$ the remanent magnetization. However, the easy coercive field was considerably smaller than H_k since the easy magnetization process were governed by magnetic domain walls displacements. Indeed, we observed charged magnetic domain walls in these CSOG films.[21] Figs. 3(e)–3(g) demonstrated the UMA exhibited by as-grown Co, Co–V and Co–Zn films.

Figure 4 shows more examples of this UMA: (a) M-H loops corresponding to an Fe–V film obtained using a mixed target ($Fe_{86}V_{14}$, target type 1), (b) Co–Fe film obtained using an alloyed target ($Co_{50}Fe_{50}$, target type 2) and (c) Fe–Al obtained using a target of sectors ($Fe_{90}Al_{10}$, target type 3). H_k was between 1000 and 1200 Oe (≈79.6–95.5 kA/m, $\mu_0 H_k \approx$ 100–120 mT). Thus, regardless of the nature of the target and film composition, all of the CSOG films display this UMA.

The origin of this magnetic anisotropy was elucidated based on the observation of the nano-sheet morphology and their corresponding top edges: these studies allowed us to establish the origin of the magnetic anisotropy of the CSOG films as a shape anisotropy generated by the growth of these tilted nano-sheets: by magnetostatic considerations, the nano-sheets forced the magnetization to be in the longitudinal direction of the nano-sheets.

Other experimental results also corroborated the origin of the anisotropic physical properties, transport, optical and magneto-mechanical, based on the particular nano-sheet morphology of the films.[22–29] Fig. 5(a) is a schematic of the home-made system for electrical resistance R measurements, showing the direction defined by the electrical contacts, the direction of the nano-sheets, and the directions in which the maximum and minimum values of R were obtained, respectively. Our works[25,29] demonstrated that all the as-grown samples exhibited an anisotropic response: R was always measured in the plane of the films, R_{min} was measured parallel to the longitudinal direction of the nano-sheets, β = 0° (180°), $R_{min} = R||$, and R_{max} was measured perpendicular to the longitudinal direction of the nano-sheets, β = 90° (270°), $R_{max} = R\perp$. For Co, $(\Delta R/R||)_{as\text{-}grown} = ([R\perp - R||]/R||)_{as\text{-}grown} \approx 24\%$, $(\Delta R/R||) \approx 33\%$ for Co–V and $(\Delta R/R||) \approx 18\%$ for Co–Zn. This anisotropic property was caused by the oriented nano-sheet morphology of the films: the electrical conduction increased when the charges moved along a nano-sheet ($R||$) with respect to the situation in which the charges moved along a perpendicular direction ($R\perp$). The mean free path of the electric charges was larger when the conduction occurred inside a nano-sheet than when the conduction was produced by traveling across the nano-sheets. Figures 5(b) and 5(c) shows the value of R (measured in the plane of the films) as a function of the angle β formed by the current and the nano-sheet longitudinal direction corresponding to a Co–Fe film obtained from an alloyed target. A clear anisotropic response is observed: Rmin = $R||$ was obtained when measured parallel to the longitudinal direction of the nano-sheet (β = 0° or 180°) and $R_{max} = R\perp$ was obtained when measured perpendicular to the longitudinal direction of the nano-sheets (β = 90° or 270°). A fit of the experimental data using the function $R(\beta) = R_{min} + \Delta R \sin^2(\beta)$ allowed obtaining the values of the parameters R_{min} and ΔR. The values of R_{min} and $R_{max} = R_{min} + \Delta R$ were assigned and the anisotropy parameter, $\Delta R/R||$, defined above as the maximum relative directional increment in resistance, was introduced. For this Co_{30}–Fe_{70} film $\Delta R/R|| \approx 136\%$.

We studied the possible influence of the films' thickness, t, on the parameter $\Delta R/R||$. For CSOG Fe films, a decrease in R with increasing t was observed, regardless of the measurement direction, as expected due to the increase in the cross section of a conductor: the higher the t, the lower the R. Remarkably, however, the value $\Delta R/R|| \approx 87\%$, remained approximately constant for all Fe films, irrespective of t (15 nm ≤ t ≤ 95 nm).[29] These two findings confirmed that the origin of the anisotropic electrical behavior was associated with the volume of the sample and not with its surface, i.e., its nano-sheet morphology, as the source of this anisotropy, was present throughout the volume of each CSOG film.

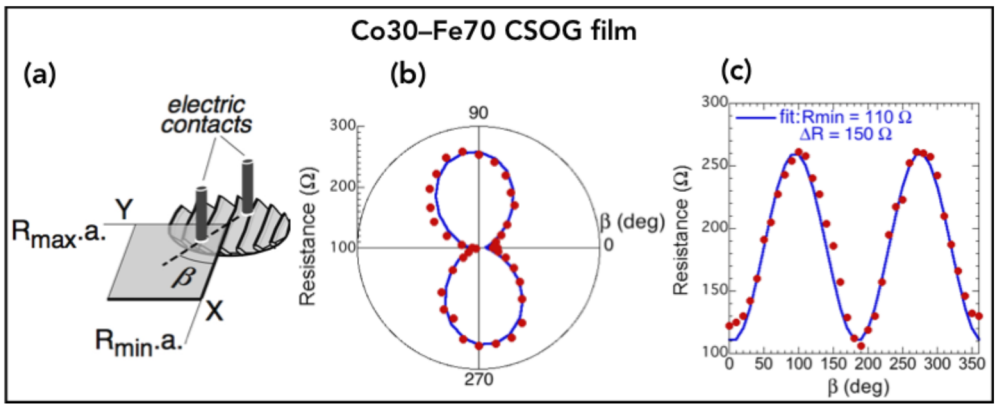

FIG. 5. (a) Schematic of the sample with the electrical contacts to measure its resistance R in the plane as a function of the angle β formed by the current and the longitudinal direction of the nano-sheets. The axes of R_{min} (β = 0° and 180°) i.e., the current parallel to the longitudinal direction of nano-sheets and R_{max} (β = 90° and 270°) i.e., the current perpendicular to the longitudinal direction of the nano-sheets are shown. (b) Experimental values, symbols, of $R(\beta)$ of a Co_{30}–Fe_{70} film in polar representation. (c) Cartesian representation of $R(\beta)$ together with its fit, solid line.

07 March 2024 09:07:32

© Author(s) 2024

Further studies were carried out on the behavior of the CSOG films after being heat treated. The first results on Co films showed that the UMA was lost simultaneously to the loss of the nano-sheet morphology.[21,25] As mentioned above, STEM images of the as-grown samples showed a regular pattern of oblique Co nano-sheets, separated approximately 1–2 nm. After annealing the film at 270 °C, although the films still displayed a pattern of oblique Co nano-entities, the separation between them decreased, and the nano-sheets tended to merge, observing a coalescence-like process.[21] This extinction of oriented nano-sheets was simultaneous with the disappearance of the uniaxial anisotropic behavior of several physical parameters, including the loss of the UMA, i.e., the disappearance of the anisotropies had its origin in the disappearance of the nano-sheets. Further annealing at 450 °C revealed no trace of nano-sheets, with the formation of *hcp* Co crystals. Similar results were found for other compositions such as Co–Zn, Co–Cd, Co–Cu. . .[27,29] The anisotropy parameter $\Delta R/R_{\|}$ was zero for these films,[25,27,28] i.e., for all of the samples whose nano-sheet morphology was not preserved after the annealing.

In contrast, other annealed films, Co–V, Co–Cr, Co–Hf and Co–Fe, retained the UMA at least up to annealing temperatures of 450–500 °C.[25,27] We demonstrated that the reason for this noteworthy behavior was the presence of the nano-sheet morphology in these annealed samples. Chemical analysis of the annealed nano-sheets showed that V was trapped by the nano-sheets favoring their maintenance.[27] Figures 6(a)–6(c) shows the HRTEM images of the

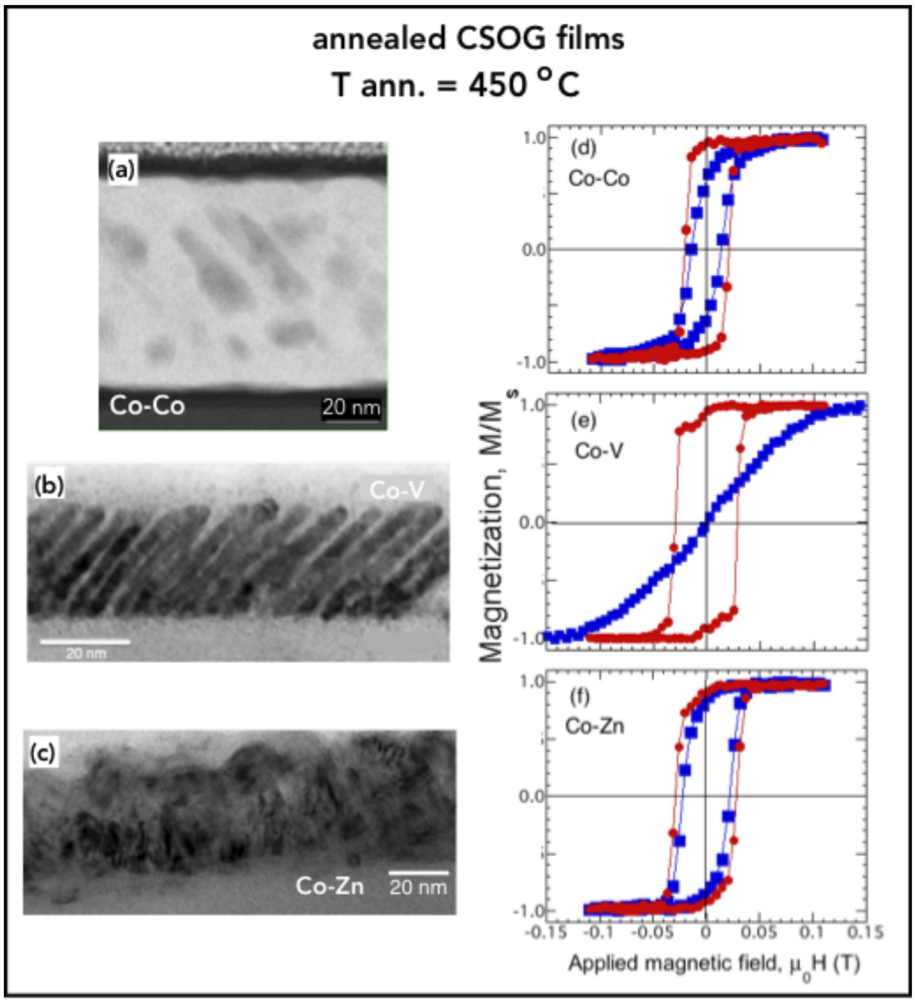

FIG. 6. HRTEM images showing the cross-sections of 450 °C annealed CSOG films. (a) Co, (b) Co–V and (c) Co–Zn. Co and Co–Zn lost the nano-sheet morphology. Co–V retained the nano-sheets. In-plane *M*–*H* hysteresis loops corresponding to these (d) Co, (e) Co–V and (f) Co–Zn CSOG films.[25–27] The hard direction (blue) and easy direction (red) are shown. If no nano-sheets were preserved, no UMA was present. Notably, in the annealed Co–V film, UMA increased as compared to the UMA of the as-grown film, Fig. 3(e). Adapted with permission from Favieres *et al.*, J. Alloy. Compd. **664**, 695 (2016). Copyright 2016 Elsevier and Adapted from Vergara *et al.*, Materials **10**, 1390 (2017); Creative Commons Attribution 4.0 International license and from Favieres *et al.*, J. Alloy. Compd. **911**, 164950 (2022); Creative Commons Attribution 4.0 International license..

07 March 2024 09:07:32

© Author(s) 2024

cross-sections of Co, Co–V and Co–Zn annealed films: for Co and Co–Zn it is clearly seen that nano-sheets no longer existed, while the Co–V annealed film retained anisotropic nano-sheet morphology (although crystals, identified as Co_3V, grew inside the nano-sheet). Figures 6(d)–6(f) shows the corresponding hysteresis loops showing the loss of UMA for the Co and Co–Zn films but a remarkable increase in $H_k \approx 79.6$ kA/m ($\mu_0 H_k = 100$ mT) for Co–V films (see for comparison the loops in Fig. 3(e), ($H_k \approx 36$ kA/m, $\mu_0 H_k = 45$ mT).

Along with the increase of the UMA in these annealed Co–V films, we observed that, despite the decrease in the R values of the annealed films, remarkably, also these films quantitatively retained the value of the anisotropy parameter $\Delta R/R\| \approx 33\%$, i.e., the percent of $(R\perp - R\|)/R\|$ was maintained, revealing that the CSOG films were, from an electrical point of view, equally anisotropic in both states, as-grown and annealed. The films' electrical conductivity was understood as exhibiting two modes: one corresponding to the nano-sheets, reflected in $R\|$, and another one associated with the inter-nano-sheet conduction.[27] This behavior is common to all the annealed samples that retained also the UMA, Co–Cr, Co–Hf, Co–Fe. . ..

IV. CONCLUSIONS

The growth and study of ferromagnetic nano-crystalline thin films constituted by a tilted nano-sheet morphology were reviewed. The visualization of these nano-sheets revealed tilt angles ≈56° with respect to the substrate plane, and nano-sheets ≈3.0–4.0 nm thick, ≈30–100 nm wide, and ≈200–300 nm long, with an inter-sheet distance ≈ 0.9–1.2 nm. The discovery of the nano-sheets allowed to elucidate the origin of the large uniaxial in-plane magnetic anisotropy exhibited by these samples, the easy direction of magnetization being parallel to the longitudinal direction of the nano-sheets. In the as-grown films, typical values of the anisotropy field were between $H_k \approx 48$ and 110 kA/m depending on composition. The changes in the nano-morphology of these films caused by thermal treatments, and hence in their anisotropic properties, were studied. HRTEM allowed the observation these morphological changes. Some films, Co–V, Co–Hf, Co–Cr, Co–Fe . . . retained their nano-sheet morphology at high temperatures, and therefore retained and even increased their anisotropies by up to three times, with anisotropy fields $H_k \approx$ 240–280 kA/m. In contrast, Co, Co–Zn, Co–Cu,. . . lost their nano-sheet-morphology. We also found large uniaxial anisotropy in other physical properties, such as the transport properties, that have been shown here.

This work opens a path of study for these new magnetically anisotropic materials, particularly with respect to the nano-morphological and structural changes related to the increase in magnetic anisotropy. A method for generating anisotropies by controlling the nano-sheet morphology of films, including oriented crystallization processes at the nano-scale, has been shown and reviewed.

ACKNOWLEDGMENTS

C. F., J. V., and V. M. acknowledge the partial financial support of the Universidad Pública de Navarra to attend the 68th Annual Conference on Magnetism and Magnetism Materials held in Dallas (TX, USA) to present the invited talk on which this work is based. C. M. and M. R. I. acknowledge the financial support from the Spanish Ministerio de Economía y Competitividad, Project No. MAT2017–82970-C1 and C2-R and from the Aragón Regional, project E26.

AUTHOR DECLARATIONS

Conflict of Interest

The authors have no conflicts to disclose.

Author Contributions

C. Favieres: Conceptualization, Investigation, Formal Analysis, Visualization, Methodology**,** Writing/Original Draft Preparation, Writing/Review & Editing. **J. Vergara**: Conceptualization, Investigation, Formal Analysis, Writing/Review & Editing. **C. Magén:** Investigation, Writing/Review & editing, **M. R. Ibarra:** Investigation, Writing/Review & editing. **V. Madurga**: Conceptualization, Investigation, Formal Analysis, Methodology**,** Visualization, Writing/Review & Editing. All authors have read and agreed to the published version of the manuscript. **V. Madurga** is an unpaid member of the Public University of Navarre.

C. Favieres: Conceptualization (equal); Data curation (equal); Formal analysis (equal); Investigation (equal); Methodology (equal); Visualization (equal); Writing – original draft (equal); Writing – review & editing (equal). **J. Vergara**: Conceptualization (equal); Formal analysis (equal); Investigation (equal); Writing – review & editing (equal). **C. Magén**: Investigation (equal); Writing – review & editing (equal). **M. R. Ibarra**: Investigation (equal); Writing – review & editing (equal). **V. Madurga**: Conceptualization (equal); Formal analysis (equal); Investigation (equal); Methodology (equal); Visualization (equal); Writing – review & editing (equal).

DATA AVAILABILITY

The data that support the findings of this study are available from the corresponding author upon reasonable request.

REFERENCES

[1] M. T. Johnson, P. J. H. Bloemen, F. J. A. D. Broeder, and J. J. D. Vries, "Magnetic anisotropy in metallic multilayers," Rep. Prog. Phys. **59**, 1409 (1996).
[2] J. W. Lau and J. M. Shaw, "Magnetic nanostructures for advanced technologies: Fabrication, metrology and challenges," J. Phys. D: Appl. Phys. **44**, 303001 (2011).
[3] G. Scheunert, O. Heinonen, R. Hardeman, A. Lapicki, M. Gubbins, and R. M. Bowman, "A review of high magnetic moment thin films for microscale and nanotechnology applications," Applied Physics Reviews **3**, 011301 (2016).
[4] A. Barman, S. Mondal, S. Sahoo, and A. De, "Magnetization dynamics of nanoscale magnetic materials: A perspective," Journal of Applied Physics **128**, 170901 (2020).
[5] Y. Shiratsuchi, M. Yamamoto, and S. D. Bader, "Magnetism and surface structure of atomically controlled ultrathin metal films," Progress in Surface Science **82**, 121–160 (2007).
[6] S. S. Rao, J. T. Prater, F. Wu, C. T. Shelton, J.-P. Maria, and J. Narayan, "Interface Magnetism in epitaxial $BiFeO_3$–$La_{0.7}Sr_{0.3}MnO_3$ heterostructures integrated on Si(100)," Nano Lett **13**, 5814–5821 (2013).

07 March 2024 09:07:32

© Author(s) 2024

[7]K. Bennemann, "Magnetic nanostructures," J. Phys.: Condens. Matter **22**, 243201 (2010).
[8]P. Poulopoulos and K. Baberschke, "Magnetism in thin films," J. Phys.: Condens. Matter **11**, 9495–9515 (1999).
[9]D. Li, D.. Pan, S. J. Li, and Z. D. Zhang, "Recent developments of rare-earth-free hard-magnetic materials," Sci. China-Phys. Mech. Astron. **59**, 617501 (2016).
[10]O. Tosun, I. Ruzybayev, F. M. Abel, B. Balamurugan, R. Skomski, D. J. Sellmyer, and G. C. Hadjipanayis, "Structural and magnetic properties of Co–V nanoparticles," AIP Advances **9**, 125144 (2019).
[11]Z. Ali, D. Basaula, W. Zhou, J. Brock, M. Khan, and K. F. Eid, "Controlling the charge transport mode in permalloy films using oblique angle deposition," Journal of Magnetism and Magnetic Materials **484**, 430–436 (2019).
[12]A. M. Aldimassi, A. Chevalier, J. Ben Youssef, V. Laur, and B. Rouvellou, "Magnetic anisotropies in oblique columnar growth of FeCoB films," AIP Advances **10**, 065218 (2020).
[13]S. S. P. M. ParkinHayashi and L. Thomas, "Magnetic domain-wall racetrack memory," Science **320**, 190 (2008).
[14]K. Bukharia, P. Karmakar, P. Pandit, and A. Gupta, "Study of magnetic nanowires of amorphous $Co_{20}Fe_{60}B_{20}$ prepared by oblique angle deposition on nanorippled substrate," Journal of Magnetism and Magnetic Materials **529**, 167842 (2021).
[15]T. G. Knorr and R. W. Hoffman, "Dependence of geometric magnetic anisotropy in thin iron films," Phys. Rev. **113**, 1039–1046 (1959).
[16]D. O. Smith, M. S. Cohen, and G. P. Weiss, "Oblique-incidence anisotropy in evaporated permalloy films," Journal of Applied Physics **31**, 1755–1762 (1960).
[17]A. Tasaki, K. Tagawa, and E. Kita, "Magnetic anisotropy of a cobalt thin film prepared by oblique incidence," Japanese Journal of Applied Physics **26**, 2037–2040 (1987).
[18]F. Liu, M. T. Umlor, L. Shen, J. Weston, W. Eads, J. A. Barnard, and G. J. Mankey, "The growth of nanoscale structured iron films by glancing angle deposition," Journal of Applied Physics **85**, 5486 (1999).
[19]J. L. Bubendorff, S. Zabrocki, G. Garreau, S. Hajjar, R. Jaafar, D. Berling, A. Mehdaoui, C. Pirri, and G. Gewinner, "Origin of the magnetic anisotropy in ferromagnetic layers deposited at oblique incidence," Europhys. Lett. **75**, 119–125 (2006).
[20]S. A. Mollick, R. Singh, B. Satpati, S. Bhattacharyya, and T. Som, "Growth angle-dependent evolution of morphology and magnetic properties of Co films on highly ordered self-organized Ge substrates," Journal of Magnetism and Magnetic Materials **498**, 166198 (2020).
[21]V. Madurga, J. Vergara, and C. Favieres, "Magnetic domain structures and nano-string morphology of laser off-normal deposited amorphous cobalt films with controlled magnetic anisotropy," Journal of Magnetism and Magnetic Materials **272–276**, 1681 (2004).
[22]V. Madurga, C. Favieres, and J. Vergara, "Growth and sculpting of Co nano-strings on Si micro-cantilevers: Magneto-mechanical properties," Nanotechnology **21**, 095702 (2010).
[23]V. Madurga, J. Vergara, and C. Favieres, "Generating and measuring the anisotropic elastic behaviour of Co thin films with oriented Surface nano-strings on micro-cantilevers," Nanoscale Research Letters **6**, 325 (2011).
[24]J. Vergara, C. Favieres, and V. Madurga, "Increased ultra high frequency magnetic susceptibility in nanopatterned nanolayers with strong exchange coupling," J. Phys. D: Appl. Phys. **48**, 435003 (2015).
[25]C. Favieres, J. Vergara, C. Magén, M. R. Ibarra, and V. Madurga, "Building oriented nano-sheets in thin films of Co–MT (MT = V, Cr, Cu, Zn, Cd, Hf) and the generation and enhancement of their magnetic anisotropy," Journal of Alloys and Compounds **664**, 695 (2016).
[26]J. Vergara, C. Favieres, C. Magén, J. M. De Teresa, M. R. Ibarra, and V. Madurga, "Structurally oriented nano-sheets in co thin films: Changing their anisotropic physical properties by thermally-induced relaxation," Materials **10**, 1390 (2017).
[27]C. Favieres, J. Vergara, C. Magén, M. R. Ibarra, and V. Madurga, "Vanadium trapped by oblique nano-sheets to preserve the anisotropy in Co–V thin films at high temperature," Journal of Alloys and Compounds **911**, 164950 (2022).
[28]C. Favieres, J. Vergara, and V. Madurga, "Tailoring magnetic and transport anisotropies in Co_{100-x}–Cu_x thin films through obliquely grown nano-sheets," Magnetochemistry **8**, 4 (2021).
[29]C. Favieres, J. Vergara, and V. Madurga, "High magnetic, transport, and optical uniaxial anisotropies generated by controlled directionally grown nano-sheets in Fe thin films," Journal of Applied Physics **133**, 124301 (2023).
[30]A. Frisk, B. Achinuq, D. G. Newman, E. Heppell, M. Dąbrowski, R. J. Hicken, G. van der Laan, and T. Hesjedal, Controlling in-plane magnetic anisotropy of Co films on MgO substrates using glancing angle deposition, Physica Status Solidi (A), **220**, 2300010 (2023).
[31]X. Jiang, J. Zhang, X. Song, H. Wang, K. Zhang, Z. He, C. Wu, Z. Yu, Z. Lan, and K. Sun, "Tunable resonance frequency of NiFe thin films by oblique deposition," Journal of Magnetism and Magnetic Materials **547**, 168946 (2022).
[32]Q. . f. Zhan, C. Van Haesendonck, S. Vandezande, and K. Temst, "Surface morphology and magnetic anisotropy of Fe/MgO(001) films deposited at oblique incidence," Applied Physics Letters **94**, 042504 (2009).
[33]D. Mukherjee, M. Hordagoda, R. Hyde, N. Bingham, H. Srikanth, S. Witanachchi, and P. Mukherjee, "Nanocolumnar interfaces and enhanced magnetic coercivity in preferentially oriented cobalt ferrite thin films grown using oblique-angle pulsed laser deposition," ACS Appl. Mater. Interfaces **5**, 7450–7457 (2013).
[34]H.-Z. Yang, M. Zeng, X.-X. Zhang, J. Liu, and R. H. Yu, "Preparation of in-plane anisotropy $Ni_{80}Co_{20}$/Bi multifilms," Rare Met **34**, 229–232 (2015).
[35]Y. Zhang, C. Huang, M. Turghun, Z. Duan, F. Wang, and W. Shi, "Electric-regulated enhanced in-plane uniaxial anisotropy in FeGa/PMN–PT composite using oblique pulsed laser deposition," Applied Physics A **124**, 289 (2018).
[36]K. Robbie, J. C. Sit, and M. J. Brett, "Advanced techniques for glancing angle deposition," Journal of Vacuum Science & Technology B: Microelectronics and Nanometer Structures Processing, Measurement, and Phenomena **16**, 1115–1122 (1998).
[37]K. Robbie, M. J. Brett, and A. Lakhtakia, "Chiral sculptured thin films," Nature **384**, 616 (1996).
[38]Y.-P. Zhao, D.-X. Ye, G.-C. Wang, and T.-M. Lu, "Designing nanostructures by glancing angle deposition," Proceedings of SPIE **5219**, 59e73 (2003).
[39]A. K. Kar, P. Morrow, X.-T. Tang, T. C. Parker, H. Li, J.-Y. Dai, M. Shima, and G.-C. Wang, "Epitaxial multilayered Co/Cu ferromagnetic nanocolumns grown by oblique angle deposition," Nanotechnology **18**, 295702 (2007).
[40]A. S. Dev, A. K. Bera, P. Gupta, V. Srihari, P. Pandit, M. Betker, M. Schwartzkopf, S. V. Roth, and D. Kumar, "Oblique angle deposited FeCo multilayered nanocolumnar structure: Magnetic anisotropy and its thermal stability in polycrystalline thin films," Applied Surface Science **590**, 153056 (2022).
[41]J. Shen, Z. Gai, and J. Kirschner, "Growth and magnetism of metallic thin films and multilayers by pulsed-laser deposition," Surface Science Reports **52**, 163–218 (2004).
[42]D. H. Lowndes, D. B. Geohegan, A. A. Puretzky, D. P. Norton, and C. M. Rouleau, "Synthesis of novel thin-film materials by pulsed laser deposition," Science **273**, 898–903 (1996).
[43]J. Schou, "Physical aspects of the pulsed laser deposition technique: The stoichiometric transfer of material from target to film," Applied Surface Science **255**, 5191–5198 (2009).
[44]Y. Hiroshima, T. Ishiguro, I. Urata, H. Makita, H. Ohta, M. Tohogi, and Y. Ichinose, "Fundamental properties in the formation of Co, Ni, and Pt metal thin films using pulsed laser deposition," Journal of Applied Physics **79**, 3572–3577 (1996).
[45]I. Horcas, R. Fernández, J. M. Gómez-Rodríguez, J. Colchero, J. Gómez-Herrero, and A. M. Baro, "Wsxm: A software for scanning probe microscopy and a tool for nanotechnology," Review of Scientific Instruments **78**, 013705 (2007).

07 March 2024 09:07:32

© Author(s) 2024